МІНЕРАЛОГІЧНИЙ ЖУРНАЛ
MINERALOGICAL JOURNAL
(UKRAINE)

UDC (549.057+549.5) : 544.77

O.M. Lavrynenko, Yu.S. Shchukin
F.D. Ovcharenko Institute of Bio-Colloid Chemistry of NAS of Ukraine
42, Acad. Vernadsky Ave., Kyiv-142, Ukraine, 03680
E-mail: alena-lavry@yandex.ru

DEVELOPMENT OF THE HYDROXYCARBONATE GREEN RUST ON THE STEEL SURFACE CONTACTING WITH WATER DISPERSION MEDIUM IN THE TEMPERATURE RANGE FROM 3 TO 70 °C

The interest in the Fe(II)–Fe(III) layered double hydroxides (LDH) or Green Rust is closely connected with the studies of the global biogeochemical cycle of iron. Its formation takes place in numerous engineering systems and in permeable reactive barriers based on iron and steel. We studied the influence of pH value (in the range from 1.5 to 11.0) and temperature (in the range from 3 to 70 °C) on the development and phase transformation of the hydroxycarbonate Green Rust on the steel (St3) surface contacting with water dispersion medium under the rotation-corrosion dispergation conditions (RCD). X-ray diffraction *in situ* and SEM were used as the main methods for the mineral phase identification. The free access of oxygen into open-air system led to solid-state transformation of GR into plates of γ-FeOOH as well as its dissolution and precipitation in well-crystalline needle-like particles of γ-FeOOH. On the contrary, the appearance of Fe_3O_4 in the phase composition of the surface structures was explained by co-precipitation of the dissolved ferric and ferrous species. The maximum quantity of γ-FeOOH phase was fixed at 25 °C and at pH 1.5 within 72 h. Maximum quantity of Fe_3O_4 phase was fixed at 70 °C and at the pH 4.0—6.5 after 24 h of the phase formation process. The crystal lattice parameters of the GR(CO_3^{2-}) formed on the steel surface within 5 h under the RCD conditions were the following: a = 0.318794, c = = 2.302260 nm (at T = 20 °C, pH 11.0) and a = 0.317084, c = 2.254410 nm (at T = 35 °C, pH 6.0).

Keywords: Fe(II)–Fe(III) layered double hydroxides, hydroxycarbonate Green Rust, lepidocrocite, magnetite, steel surface, the rotation-corrosion dispergation conditions.

Introduction. The interest in the Fe(II)–Fe(III) layered double hydroxides (LDH) or their natural analogues called Green Rust [11] is closely connected with the studies of the global biogeochemical cycle of iron [38]. The identification of a Green Rust as a mineral was performed in waterlogged soils of "gleyic properties" under forest in Fougeres (Brittany, France) [36]. The recent identification of Green Rusts as products of the ferric oxide and oxyhydroxide reduction by *Shewanella putrefaciens* [27], a dissimilatory iron-reducing bacterium (DIRB) [13, 39], suggests that Green Rusts are the intrinsic component of the iron red-ox cycle in aquatic and terrestrial environments [26].

The formation of the Green Rust takes place in numerous engineering systems [35] and in permeable reactive barriers based on iron and steel [18]. Usually electrochemical synthesis of Fe(II)–Fe(III) LDH is used for modeling of the atmospheric corrosion process [25] as well as a marine one [33].

Nowadays the crystal structure of Fe(II)–Fe(III) LDH is well known and it is described as positively charged brucite-like layers $[Fe^{II}_{(1-x)}Fe^{III}_{x}(OH)_2]^{x+}$ that alternate with interlayers made of anions and water molecules [11]. The type of Green Rust structure is determined by the shape and type of anions they incorporate. Whereas iron hydroxide layers in the Green Rust I are coordinated by "planar" or "spherical" anions such as Cl^-, F^-, I^-, CO_3^{2-}, SO_3^{2-}, Green Rust II is formed in the presence of "three-dimensional" anions such as SO_4^{2-} or SeO_4^{2-} [14, 16]. Green Rust I (GRI) with hydrotalcite-like $([Mg^{II}_4Al^{III}_2(OH)_{12}]^{2+}\cdot [CO_3^{2-}, 3H_2O]^{2-}$ [9] or pyroaurite-like $([Mg^{II}_6Fe^{III}_2 \times \times (OH)_{16}]^{2+}$ $[CO_3^{2-}, \sim 4H_2O]^{2-}$ [8]) XRD pattern belongs to the hexagonal system; its space group is $P\bar{3}m$. The structure of Green Rust II is close to

Редколегія усвідомлює, що тема даної статті не відповідає тематиці "Мінералогічного журналу", однак отримані авторами результати можуть бути цікавими для мінералогів.

that of $Fe(OH)_2$ and it belongs to the trigonal system with space group $P\bar{3}m1$ [14].

Despite of the fact that crystal lattice parameters, structure and physical-chemical properties of Green Rusts are determined, they may strongly depend on the following external factors: the method of the LDH obtaining, chemical composition and pH value of dispersion medium, temperature, *red-ox* conditions, duration of the phase formation process etc. Recently we proposed a new rotation-corrosion dispergation (RCD) method [20], that permits to form different iron-oxygen structures including Fe(II)–Fe(III) LDH on the steel surface alternately contacting with water dispersion medium and air.

The purpose of our work is to study the influence of pH value and temperature on the development and phase transformation of the hydroxycarbonate Green Rust on the steel surface contacting with dispersion medium under the rotation-corrosion dispergation conditions.

Objects and methods of the research. The formation of the Green Rust applying the rotation-corrosion dispergation method was carried out on the surface of the rotating disk electrode made of the finished steel (St3). Its chemical composition is the following, %: C — 0.14—0.22; Si — 0.05—0.15; Mn — 0.4—0.65; Cr — 0.3; Ni — 0.3; P — 0.04; S — 0.05; N — 0.01. Such steel appears to be the iron-carbon alloy containing the phases of iron spinel ferrite $FeFe_2O_4$, graphite C and cementite $(Fe, Ni, Co)_3C$. Due to the presence of such components, a large number of micro galvanic couples, such as ferrite — graphite and ferrite — cementite, are created in the system. In these couples, the ferrite particles play the role of anodes whereas the graphite and cementite particles are cathodes. The differences in the value of standard electrode potentials of such components lead to the electrochemical red-ox reactions on the steel surface. As it was shown in our earlier article [2], the additional components of steel, such as Si, Mn, Cr, Ni, Cu, S, P, do not participate in the processes of the phase formation: their concentration in the dispersion medium is very low. The rotation of the steel disk supplies the variable contact of its surface with air and dispersion medium. The process of the phase formation was carried out in *the open-air system*.

The steel surface was refined from oxidized layer via mechanical and chemical treatment. The sulfate acid water solution (1 : 1) was used as a chemical agent for the surface activation. The electrode washed off with distilled water was many times. Distilled water (pH 6.5) was chosen as a dispersion medium. To prepare water solutions in the wide range of pH (from 1.5 to 11.0) the respective quantity of HCl (1 : 1) and NaOH (1 M) was added into distilled water. The pH value in the solutions was controlled using ion meter (*И* 160, made in Belarus). The temperature regimes were provided by applying of TS-1/80-SPU thermostat. The obtaining of the surface structures was carried out at the following temperatures: 3, 10, 25, 35, 50 and 70 °C. The process of the phase formation led to the stationary state of the system (48—72 h).

X-ray diffraction (XRD) was used for the mineral phase identification. We used the XRD *in situ* study to fix the processes of the iron-oxygen particle development and their phase transformation on the steel [19]. The measurement was taken on computer-aided equipment (DRON 3) with filtered emission of a cobalt anode in discrete conditions of plotting, with the pitch of 0.1 degree and time of piling in every point 4 s. The crystal lattice parameters of mineral phases and the primary particle size (coherent scattering region, CSR), were calculated according to XRD-data [1]. The relative quantity of the mineral phase and the kinetic regularities were obtained applying the method [5]. As an additional visualization technique of the derived samples a scanning electron microscopy (SEM) was suggested.

Result and discussion. *The influence of the pH value on the development of Green Rust I on the steel surface under the rotation-corrosion dispergation conditions*. The study of the mineral composition of the surface structures formed under the RCD conditions on the steel surface was carried out using XRD analysis *in situ* (Fig. 1). According to the obtained data Green Rust I, lepidocrocite γ-FeOOH and magnetite Fe_3O_4 formed in the wide range of pH (from 1.5 to 11.0) at T = 25 °C and pH 6.5 as the main mineral phases.

Only lepidocrocite was formed on the steel surface when it was contacting with water dispersion medium at pH 1.5. The first lepidocrocite peaks (020) and (120) appeared within 2 h. Their quantity and intensity gradually increased during 72 h. The increase of the initial pH value to 4.0 led to the appearance of lepidocrocite reflexes within 1 h of the process. The formation of the magnetite on the steel surface was fixed after 5 h from the start of the phase formation process. Their intensity was three times grown within 48 h. The emergence of the lepidocrocite at pH 6.5 was noticed during 2 h and magnetite was formed in 5 h. At the same time the accumulation of the magnetite phase took place

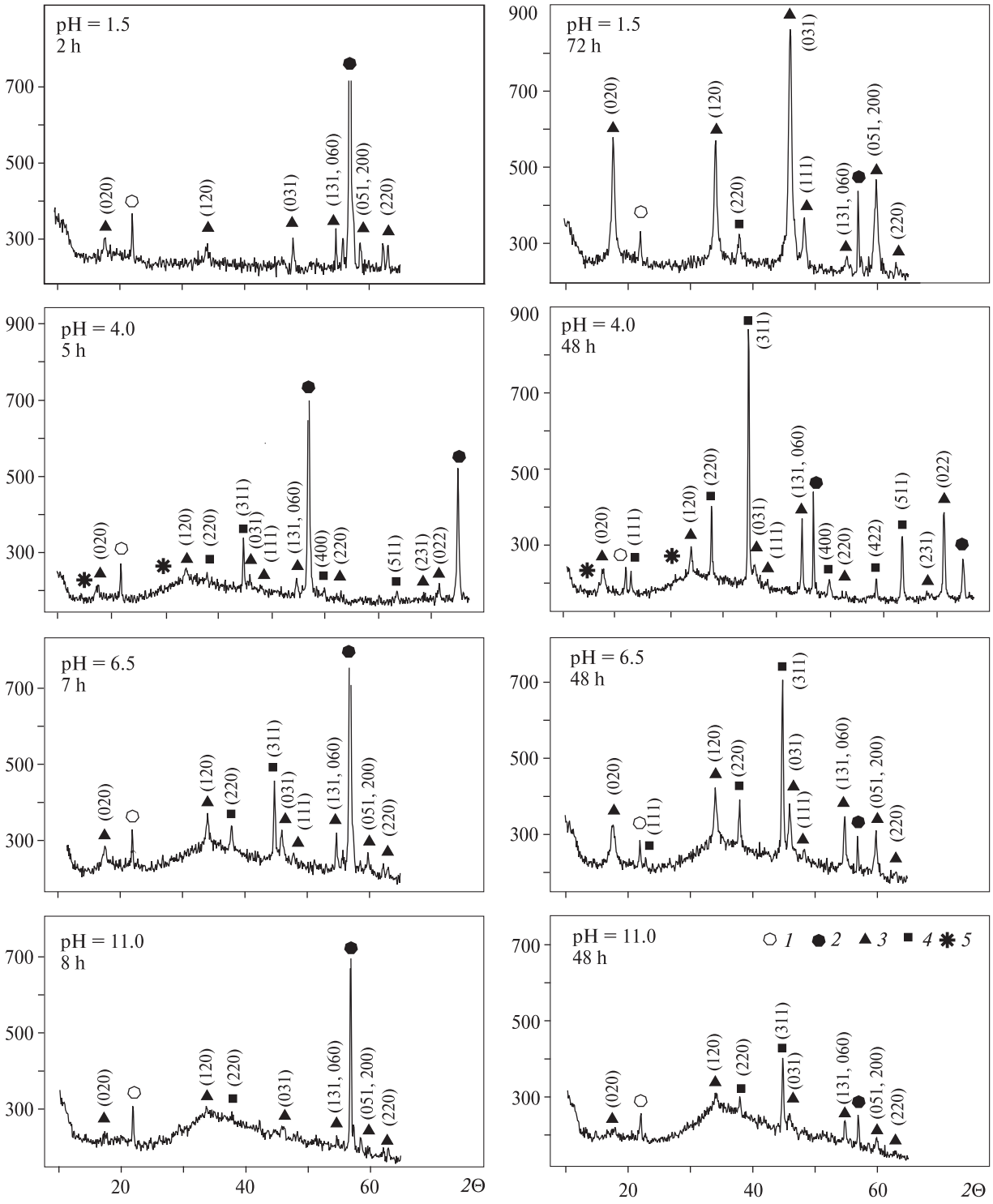

Fig. 1. XRD-patterns obtained under *in situ* condition when the steel surface was contacting with water solution in the pH range from 1.5 to 11.0. The numbers correspond to the mineral phases: *1* — goethite, *2* — iron (the steel surface), *3* — lepidocrocite, *4* — magnetite, *5* — Green Rust I

more intensively than lepidocrocite. The system came to the stationary state after 48 h. The reflexes of the lepidocrocite formed at pH 11.0 were very weak. And the first reflexes of magnetite (311) and (220) appeared after 24 h of the phase formation process and their intensity insignificantly increased. It is indicative that the XRD peaks of Green Rust I were clearly seen only at the pH 1.5 (7 h) and at the pH 11.0 (2—8 h). Obviously in the acid medium the iron hydroxide layers in the Green Rust I

structure were coordinated by chloride anions and it may belong to hydroxdylchloride Green Rust GR(Cl^-). But in alkaline medium Green Rust I could be only hydroxycarbonate GR(CO_3^{2-}). The crystal lattice parameters of the Green Rust I formed on the steel surface under RCD conditions are the following: a = 0.322379, c = 2.452110 nm for GR(Cl^-) (pH 1.5, 7 h) and a = 0.318794, c = = 2.302260 nm for GR(CO_3^{2-}) (pH 11.0, 5 h).

So, according to the obtained data the influence of the pH value on the phase composition of the surface structures in the pH range from 4.0 to 10.0 is not significant because it is compensated by cathode process due to the neutralization of the solution in the reaction area [2]. That leads to the formation of the stable mineral compositions on the steel surface that includes lepidocrocite and magnetite. On the contrary the quantity of the products of cathode process in highly acidic and highly alkaline medium is not enough for neutralization of pH in the reaction area and weak crystallized phases such as Green Rust and lepidocrocite are preferentially formed on the steel surface.

We used the XRD patterns for the comparison of the relative quantity of lepidocrocite and magnetite formed in the pH range from 1.5 to 11.0. The obtained data (Table 1) show that the maximum quantity of lepidocrocite is formed at pH 1.5 within 72 h. But the maximum of magnetite is fixed in the pH range from 4.0 to 6.5 after 24 h of the phase formation process.

The average size of the primary magnetite particles calculated using the Debay-Scherrer formula is gradually increased together with the increase of pH value and it equals ~20.8 nm at pH 4.0, ~26.4 at pH 6.5 and ~31.0 at pH 11.0. The average length of lepidocrocite needles is increased too when the initial pH value grows. It equals ~18.3 nm at pH 1.5, ~19.4 at pH 4.0, ~20.0 at pH 6.5 and ~26.2 nm at pH 11.0.

The influence of the temperature on the development of hydroxycarbonate Green Rust on the steel surface under the RCD conditions. The role of the temperature in the phase composition of mineral phases formed on the steel surface was studied using XDR analysis in situ (Fig. 2) and scanning electron microscopy (Fig. 3). The formation of the mineral particles was carried out in the temperature range from 3 to 70 °C. All minerals formed under experimental conditions belong to the iron-oxygen structural γ-row: hydroxycarbonate Green Rust GR(CO_3^{2-}), lepidocrocite γ-FeOOH and magnetite Fe_3O_4. The quantity of goethite α-FeOOH was insignificant and it can be estimated as an additional phase.

The lepidocrocite reflexes appeared on the steel surface at T = 3 °C within 72 h and γ-FeOOH remained as a single phase until the system came to the stationary state. The increase of the temperature to 10 °C led to appearance lepidocrocite together with magnetite Fe_3O_4 within 48 h. The formation of both phases γ-FeOOH and Fe_3O_4 at T = 25 °C was fixed after 2 h of the process. The intensity of their reflexes gradually increased within 72 h. The first reflexes of γ-FeOOH and Fe_3O_4 appeared at T = 35 °C after 2 h of the phase formation. The intensity of the γ-FeOOH reflexes was growing during 10 h and then it did not change within next 62 h. But the intensity of the Fe_3O_4 reflexes gradually increased, reached its maximum within 48 h and further it decreased by the end of the experiment (72 h). Hydroxycarbonate Green Rust GR(CO_3^{2-}) and goethite α-FeOOH were fixed using X-ray diffraction method at T = 35 °C. The intensity of lepidocrocite reflexes was increasing at T = 50 °C during all experiment, but the intensity of magnetite peaks reached its maximum within 48 h and then it insignificantly decreased. The strong reflexes of γ-FeOOH and Fe_3O_4 together with weak reflexes of α-FeOOH were present on the XRD pattern at T = 70 °C. The intensity of the γ-FeOOH and

Table 1. **The relative quantity of the mineral phases formed on the steel surface contacted with water disperse medium in the pH range from 1.5 to 11.0**

pH value	Time, h	Phases	
		γ-FeOOH	Magnetite
1.5	2	0.16	0.00
	7	0.11	0.05
	24	0.47	0.10
	48	0.74	0.10
	72	**1.00**	0.11
4.0	0.5	0.00	0.00
	1	0.00	0.00
	5	0.08	0.19
	9	0.15	0.55
	24	0.23	**1.00**
	48	0.15	0.66
6.5	2	0.23	0.27
	7	0.23	0.27
	24	0.46	0.80
	48	0.26	0.66
	55	0.39	0.72
11.0	2	0.00	0.00
	5	0.00	0.00
	8	0.08	0.02
	24	0.06	0.10
	48	0.08	0.22

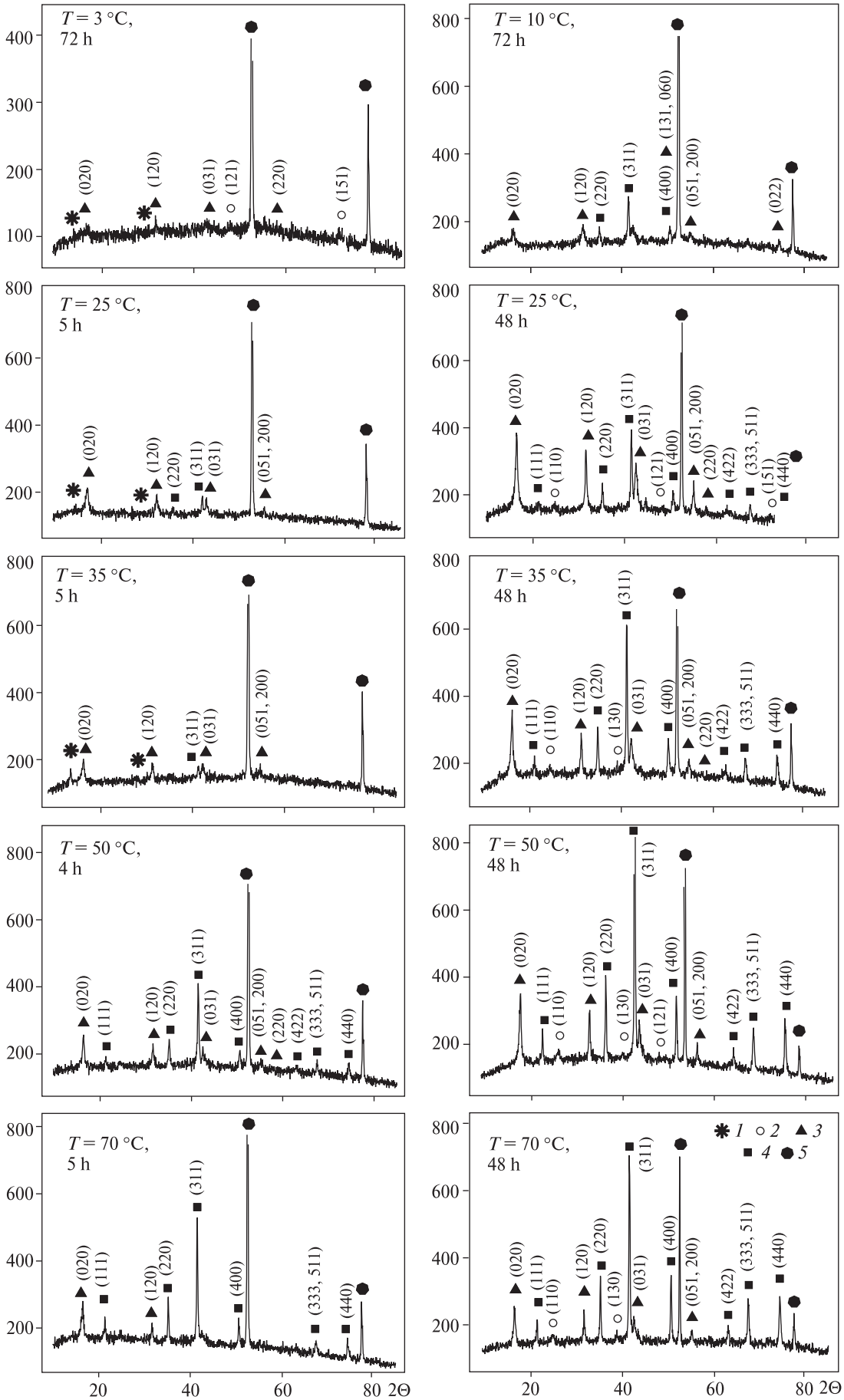
T = 3 °C, 72 h
(020)
(120)
(031)
(121)
(220)
(151)
T = 10 °C, 72 h
(020)
(120)
(220)
(311)
(400)
(131, 060)
(051, 200)
(022)
T = 25 °C, 5 h
(020)
(120)
(220)
(311)
(031)
(051, 200)
T = 25 °C, 48 h
(020)
(111)
(110)
(120)
(220)
(311)
(031)
(121)
(400)
(051, 200)
(220)
(422)
(333, 511)
(151)
(440)
T = 35 °C, 5 h
(020)
(120)
(311)
(031)
(051, 200)
T = 35 °C, 48 h
(020)
(111)
(110)
(120)
(220)
(130)
(311)
(031)
(400)
(051, 200)
(220)
(422)
(333, 511)
(440)
T = 50 °C, 4 h
(020)
(111)
(120)
(220)
(311)
(031)
(400)
(051, 200)
(220)
(422)
(333, 511)
(440)
T = 50 °C, 48 h
(020)
(111)
(110)
(120)
(220)
(130)
(311)
(031)
(121)
(400)
(051, 200)
(422)
(333, 511)
(440)
T = 70 °C, 5 h
(020)
(111)
(120)
(220)
(311)
(400)
(333, 511)
(440)
T = 70 °C, 48 h
1 2 3 4 5
(020)
(111)
(110)
(120)
(220)
(130)
(311)
(031)
(400)
(051, 200)
(422)
(333, 511)
(440)
20
40
60
80 2Θ

Fig. 2. XRD-patterns obtained under *in situ* condition when the steel surface was contacting with water solution in the temperature range from 10 to 70 °C. The numbers correspond to the mineral phases: *1* — Green Rust I, *2* — goethite, *3* — lepidocrocite, *4* — magnetite, *5* — iron (the steel surface) ◀

Fe_3O_4 reflexes increased within 9 and 18 h, respectively and further it gradually decreased. The most intensive reflexes of α-FeOOH were fixed after 9 h of the phase formation process, and further their intensity did not changed.

The magnetite particles formed on the steel surface in the wide temperature range (35—70 °C) have a spherical shape (Fig. 3, *h*, *g*, *m*) and nanosized scale of CSR. The increase of the temperature in the system leads to decrease of the particle size. So, the average size of magnetite particles formed at $T = 10$ °C equals ~28.0 nm; at $T = 25$ °C — 24.6; at $T = 35$ °C — 24.4; at $T = 50$ °C — 18.7; at $T = 70$ °C — 17.9 nm. On the contrary the length of the lepidocrocite needles gradually grows when the phase formation temperature increases. Their average size equals ~20.0 nm at $T = 10$ °C; ~24.4 at $T = 25$ °C; ~28.5 at $T = 35$ °C; ~34.0 at $T = 50$ °C and ~36.0 nm at $T = 70$ °C. The crystal lattice parameters of the Green Rust I formed on the steel surface under the RCD conditions at $T = 35$ °C within 5 h are the following: $a = 0.317084$, $c = 2.254410$ nm.

The comparison of the relative quantity of lepidocrocite and magnetite formed in the all temperature range is presented in Table 2. According to the obtained data the quantity of lepidocrocite reaches its maximum in the temperature range from 25 to 50 °C within 48 h of the phase formation process. It is indicative that magnetite phase is absent at $T = 10$ °C even after 72 h of the process. The relative quantity of magnetite gradually increased in all temperature range and it reached maximum at 70 °C within 18 h. Further its quantity was insignificantly decreased.

The SEM images of the surface structures formed in the temperature range from 10 to 70 °C are present on Fig. 3. So, the randomly oriented plates of hydroxycarbonate Green Rust (Fig. 3, *a*) and the needles of lepidocrocite (Fig. 3, *b*) are clearly seen on the steel surface after 72 h of the phase formation process at $T = 10$ °C. Distorted lepidocrocite needles formed within 10 h at $T = 25$ °C are present on Fig. 3, *c*. Spherical magnetite particles obtained under such conditions on the steel surface are seen on Fig. 3, *d*. The general view of the iron-oxygen structures formed in and around the structural defect on the steel surface is present on Fig. 3, *e*. The oriented lepidocrocite needles precipitated on the steel surface within 10 h at $T = 35$ °C are seen on Fig. 3, *f*. The "hedge-hog" structures of schwertmannite formed under such conditions are present on Fig. 3, *g* and magnetite particles are seen on Fig. 3, *h*. The following particles are formed within 5 h at $T = 50$ °C on the steel surface: lepidocrocite (Fig. 3, *i*) and magnetite (Fig. 3, *j*). The lepidocrocite particles obtained within 4 h at $T = 70$ °C are present on Fig. 3, *k*. The "hedge-hog" structures of schwertmannite formed under the same conditions are seen on Fig. 3, *l*. The magnetite particles (Fig. 3, *m*) and its "rod-like" aggregates (Fig. 3, *n*) were formed simultaneously with γ-FeOOH at $T = 70$ °C.

The colloidal-chemical mechanisms of the formation of Green Rust I on the steel surface contacting with air oxygen and water solutions. The formation of the Fe(II)—Fe(III) layered double hydroxides (LDH) or Green Rust takes place on the steel surface when the dissolved ferrous iron as well as hydroxyl, oxygen, carbon-oxygen and some anion species are present in the water solution contacting with the steel.

As it was shown in our previous work [2], the average pH value in the reaction area can lie in the

Table 2. **The relative quantity of the mineral phases formed on the steel surface contacted with water disperse medium in the temperature range from 10 to 70 °C**

Temperature, °C	Time, h	Mineral phases	
		γ-FeOOH	Fe_3O_4
10	1	0.00	0.00
	2	0.00	0.00
	5	0.00	0.00
	48	0.00	0.00
	72	0.15	0.17
25	2	0.00	0.00
	5	0.33	0.06
	25	0.95	0.20
	48	**1.00**	0.23
35	5	0.28	0.03
	10	0.89	0.27
	48	0.82	0.51
50	4	0.42	0.28
	21	0.54	0.76
	48	0.96	0.95
70	1	0.11	0.15
	5	0.44	0.42
	18	0.57	**1.00**
	48	0.47	0.76

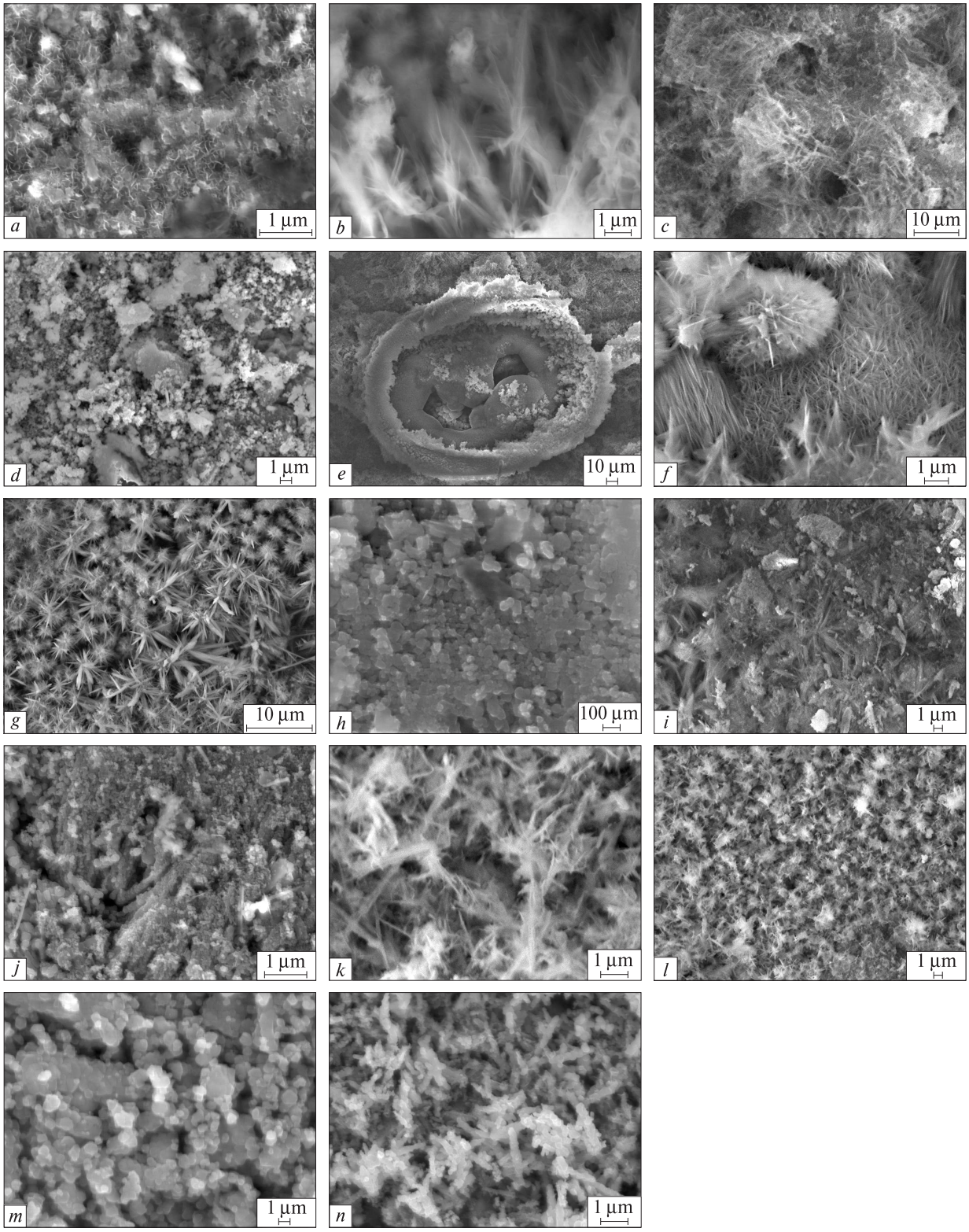

Fig. 3. The SEM images of the iron-oxygen minerals formed on the steel surface contacted with distilled water at $T = 10$ °C: *a* — GR(CO_3^{2-}), *b* — γ-FeOOH; at $T = 25$ °C: *c* — γ-FeOOH, *d* — Fe_3O_4, *e* — the structural defect of the steel; at $T = 35$ °C: *f* — γ-FeOOH, *g* — schwertmannite, *h* — Fe_3O_4; at $T = 50$ °C: *i* — γ-FeOOH, *j* — Fe_3O_4; at $T = 70$ °C: *k* — γ-FeOOH, *l* — schwertmannite, *m* — Fe_3O_4 particles, *n* — "rod-like" aggregates of Fe_3O_4

range from 7.0 to 9.5 independently on the pH in the volume of the solutions. We confirmed such data using the direct test with the help of the corresponding indicators (*nitrasin yellow* and *phenolic red*) [21]. The narrow pH range is the cause of the limited quantity of the iron (ferrum) aquahydroxoforms in the reaction area. So, ferric iron is precipitated as an amorphous hydroxide $Fe(OH)_3$, and ferrous iron can exist in form of hydrated cations Fe^{2+}, aquahydroxocomplexes $FeOH^+$ and hydroxide $Fe(OH)_2$. Hydroxyl and protons are other active components in the reaction area. Oxygen and oxygen-bearing carbon compounds (OBCC) enter into the interface *the steel surface — water dispersion medium* from air and they are stepwise adsorbed on the steel surface [7]. The OBCC can exist in the *open-air system* as carbon dioxide CO_2 or carbonic acid H_2CO_3 as well as the anions — HCO_3^-, CO_3^{2-}, that can interact with dissolved iron (ferrum) and form different dissolved complexes, e. g. $FeHCO_3^+$, $Fe(HCO_3)_2$, $Fe(CO_3)_2^{2-}$ [23].

Under such conditions the formation of the peculiar micellar structures in the reaction area (~ 400 mkm from steel surface) is possible after a few minutes of the contact of the electrode with the dispersion medium.

In the presence of dissolved ferrous aquahydroxoforms the micelle composition can be the following [3]:

$$\{[m\mathrm{Fe(OH)_2}]\cdot n\mathrm{FeOH^+}\cdot (n-x)\mathrm{OH^-}\}^{x+}\cdot x\mathrm{OH^-}$$

or

$$\{[m\mathrm{Fe(OH)_2}]\cdot n\mathrm{Fe^{2+}}\cdot 2(n-x)\ \mathrm{OH^-}\}^{2x+}\cdot 2x\mathrm{OH^-}.$$

But when both ferrous and ferric aquahydroxoforms are present in the system the micelle composition is different [3]:

$$\{[m\mathrm{Fe(OH)_3}]\cdot 2n\mathrm{FeOH^+}\cdot (n-x)A^{2-}\}^{2x+}\cdot xA^{2-}$$

or

$$\{[m\mathrm{Fe(OH)_3}]\cdot n\mathrm{Fe^{2+}}\cdot (n-x)A^{2-}\}^{2x+}\cdot xA^{2-}.$$

The letter A^{2-} corresponds to SO_4^{2-}, CO_3^{2-} anions.

We think that such micellar structures are the precursor species for the Green Rust formed on the steel surface. That supposition agrees with the electrochemical researches [15, 34] where the gel-like phase $Fe(OH)_2$ appears on the iron surface under corrosion conditions. Moreover, on the first stage of corrosion process at pH 4.0—9.5 the steel surface contacts with alkaline water solution saturated with relation to the $Fe(OH)_2$ protective layer [6].

The compromise potential of the steel electrode was found in the range from −0.6 to −0.3 V, and it permitted the origin of the primary Green Rust particles on the steel surface [28].

The general reactions of the hydroxycarbonate Green Rust formation can be the following [3]:

$$3\mathrm{Fe(OH)_2} + 3[\mathrm{Fe(OH)_{(x)}}]^{[2-x]+} + \mathrm{H_y(CO_3)^{(2-y)-}} + (8-3x)\mathrm{H_2O} + 0.5\mathrm{O_2} = \mathrm{Fe^{II}{}_4Fe^{III}{}_2(OH)_{12}CO_3}\cdot 3\mathrm{H_2O} + (4-3x+y)\mathrm{H^+}, \quad (1)$$

or

$$2\mathrm{Fe(OH)_3} + 4[\mathrm{Fe(OH)_{(x)}}]^{[2-x]+} + [\mathrm{H_y(CO_3)}]^{[2-y]-} + (9-4x)\mathrm{H_2O} = \mathrm{Fe^{II}{}_4Fe^{III}{}_2(OH)_{12}CO_3}\cdot 3\mathrm{H_2O} + (6-4x+y)\mathrm{H^+}, \quad (2)$$

where $x = 0, 1$; $y = 0, 1, 2$.

The electrochemical synthesis of hydroxycarbonate Green Rust $[Fe_4^{II}Fe_2^{III}(OH)_{12}]^{2+}\cdot[CO_3\cdot 2H_2O]^{2-}$ on the brushed up surface of the iron electrode (99.5 % Fe^0) contacting with complex electrolyte (0.2 M water solution NaCl + $NaHCO_3$ + NaOH at pH 9.6 and T = 25 °C) was realized under potentiostatic oxidation at E = −0.72 V [16]. The obtained data show the simultaneous entry of carbonate and chloride anions into Green Rust structure. The formation of the $GR(CO_3^{2-})$ in the water solutions includes two stages: 1) the formation of GR at $E = -0.75 \div -0.6$ and 2.0 V Green Rust oxidation at E = −0.3 V [15]. The capability of ferrous iron of chemical and electrochemical oxidation, further co-precipitation with ferric species and formation of GR structure were shown in [30]. The oxidation of ferrous iron in the crystal lattice of $Fe(OH)_2$ accompanied by CO_3^{2-} intercalation is considered to be less likely [16].

Two principle approaches to the Green Rust formation via electrochemical synthesis exist: the change of the local pH value or the degree of ferrum oxidation (Fe(II), Fe(II) + Fe(III), Fe(III)) [28]. In the first case the near electrode area is alkalinized e. g. due to the reduction of the dissolved oxygen or water and hydroxyl disengagement [17]. It leads to the formation of the iron-oxygen structures on the electrode surface. The formation of the concomitant structures of iron oxides and hydroxides may be related to the limitation of a method. In the second case the anodal oxidation of electrodeposited GR layer on the gold and silver electrodes is realized at pH 9.5 and I = 16.7 mA·cm^{-2} [29]. The oxidation of the GR layer was fixed at E = −0.5 V. The increase of temperature (T > 50 °C) led to the formation of the monophase ferric oxyhydroxycarbonate $Fe_6O_2(OH)_{12}CO_3$. The solid state reaction of the

anodal oxidation of $GR(CO_3^{2-})$ was characterized by anodal peak at $E = -0.32$ V. Cathodal solid state reduction of $Fe_6O_2(OH)_{12}CO_3$ into $GR(CO_3^{2-})$ was realized at $E = -0.48$ V. The ratio of $R =$ = Fe(II)/Fe(III) for $GR(CO_3^{2-})$ equals ~2.0—2.5 [37]. Green Rust as well as ferric (oxy)hydroxycarbonate formed in the phase composition at $R > 2.0$.

Temperature belongs to the critical parameter for the formation of hydroxycarbonate Green Rust on the steel/iron surface because the concentration of carbonate species (CO_2) forms the inverse correlation in relation to temperature (from 0.232 per 100 g water at $T = 10$ °C to 0.058 per 100 g water at $T = 60$ °C to complete disappearance at $T > 65$ °C) [4]. So, it may be important for the interpretation of our experimental data about further Green Rust transformation.

Only two mineral phases were determined according to XRD data obtained *in situ*: lepidocrocite and magnetite. The electrochemical mechanism of the GR transformation into γ-FeOOH includes dissolution of Green Rust particles and further formation of the primary particles of γ-FeOOH on the whole electrode surface [10, 22]. Whereas the oxidation of Green Rust can lead to the formation of magnetite particles as an intermediate product of the reaction that is included into GR crystal lattice or it may replace the structural elements in the GR [31]. The further oxidation leads to destruction of both kinds of particles and precipitation of the needle-like lepidocrocite.

The chemical mechanism of the magnetite formation in the Green Rust water suspension as a rule is realized via Green Rust dissolution and further precipitation of Fe_3O_4 particles [32]. The presence of ferrous cations in the open-air system can cause the formation of initial ferryhydrite particles. The rate of GR dissolution increases at the increasing of the pH value in the suspension. Dissolved ferrous iron is gradually oxidized and forms ferric oxyhydroxide phase [24].

Also, as the more probable mechanisms of the phase formation on the steel surface under rotation-corrosion dispergation conditions we determined the following: the $GR(CO_3^{2-})$ oxidation into γ-FeOOH (3) and the formation of magnetite particles via dissolved ferrous and ferric micellar species interaction

$$Fe^{II}_4Fe^{III}_2(OH)_{12}CO_3 \cdot nH_2O + O_2 \rightarrow$$
$$\rightarrow 6\gamma\text{-}FeOOH + H_2CO_3 + (2 + n)H_2O. \quad (3)$$

We explain the formation of schwertmannite $Fe_8O_8(OH)_{8-2x}(SO_4)_x$ particles [12] on the steel surface as a result of the interaction of ferrous iron and hydroxyl with the "trace" amount of SO_4^{2-} that may remain in the defects of the steel after its chemical activation.

Conclusions. The contact of the steel surface with water dispersion medium under the rotation-corrosion dispergation conditions leads to the formation of the disperse iron-oxygen minerals including Fe(II)—Fe(III) layered double hydroxides, lepidocrocite and magnetite. The physical-chemical conditions such as pH value of dispersion medium and temperature play an important role in the phase distribution on the steel surface. The optimal conditions for the formation of hydroxychloride Green Rust were fixed at pH 1.5 but for the formation of hydroxycarbonate one it was found at pH 11.0. We determined the most quantity of $GR(CO_3^{2-})$ within 5 h when the phase formation process took place in the temperature range 25—35 °C.

The presence of ferrous iron in a crystal lattice of Green Rusts causes their oxidation, dissolution and phase transformation. The free access of oxygen into our open-air system leads to solid-state transformation of GR into plates of lepidocrocite as well as its dissolution and precipitation in well-crystalline needle-like particles of lepidocrocite. On the contrary, the appearance of magnetite in the phase composition of the surface structures is explained by dissolved ferric and ferrous species co-precipitation.

The comparison of the XRD-peak intensity permits to estimate relative quantity lepidocrocite and magnetite formed in the pH range from 1.5 to 11.0 and in the temperature range from 10 to 70 °C. Whereas the quantity of lepidocrocite gradually increases within the temperature range from 10 to 50 °C and it is identified as a monophase at $T =$ = 10 °C, magnetite quantity grows in the all temperature range. The maximum of γ-FeOOH phase is fixed at 25 °C and maximum of Fe_3O_4 phase is fixed at 70 °C, respectively. The maximum quantity of lepidocrocite is formed at pH 1.5 within 72 h and the magnetite quantity reaches its maximum in the pH range from 4.0 to 6.5 after 24 h of the phase formation process.

We acknowledge leading research scientist, candidate of geological and mineralogical sciences O.A. Vyshnevskyi of Mass-spectrometric centre of solidphase, gas isotopic trace element analysis (M.P. Semenenko Institute of Geochemistry, Mineralogy and Ore Formation of NAS of Ukraine) for the obtaining of the SEM images and EDS data.

REFERENCES

1. *Гинье А.* Рентгенография кристаллов : Пер с фр. — М. : Физматгиз, 1961. — 604 с.
2. *Лавриненко Е.Н.* Роль катионов железа дисперсионной среды при образовании железо-кислородных структур в системах на основе железа и углерода // Наносистеми, наноматеріали, нанотехнології. — 2008. — **6**, спец. вип. 2. — С. 529—550.
3. *Лавриненко О.М.* Одержання композиційних структурованих систем на основі ферум-оксигенвмісних мінералів, їх структура та властивості : Автореф. дис. ... д-ра хім. наук. — К., 2013. — 40 с.
4. *Лурье Ю.Ю.* Справочник по аналитической химии. — 6-е изд. перераб. и доп. — М. : Химия, 1989. — 448 с.
5. *Прокопенко В.А., Лавриненко Е.Н., Ващенко А.А., Надел Л.Г.* Адаптация традиционных физико-химических методов разделения для дисперсных фаз железо-кислородных соединений // Экотехнологии и ресурсосбережение. — 2005. — № 6. — С. 36—42.
6. *Эванс Ю.Р.* Коррозия и окисление металлов (Теоретические основы и их практическое применение) : Пер. с англ. — М. : Машгиз, 1962. — 856 с.
7. *Юнг Л.* Анодные оксидные пленки : Пер. с англ. — Л. : Энергия, 1967. — 232 с.
8. *Allmann R.* The crystal structure of pyroaurite // Acta Crystallogr. B. — 1968. — **24**. — P. 972—977.
9. *Allmann R., Jepsen H.P.* Die Struktur des Hydrotalkits // Neues Jahrb. Mineral. Monatsh. — 1969. — **B12**. — P. 544—551.
10. *Antony H., Peulon S., Legrand L., Chausse A.* Electrochemical synthesis of lepidocrocite thin films on gold substrate — EQCM, IRRAS, SEM and XRD study // Electrochim. Acta. — 2004. — **50**. — P. 1015—1021.
11. *Bernal J.D., Dasgupta D.R., Mackay A.L.* The oxides and hydroxides of iron and their structural inter-relationships // Clay Miner. Bull. — 1959. — **4**. — P. 15—30.
12. *Bigham J.M., Schwertmann U., Traina S.J., Winland R.L., Wolf M.* Schwertmannite and the chemical modelling of iron in acid sulphate waters // Geochim. et cosmochim. acta. — 1996. — **60**. — P. 2111—2121.
13. *Duan J., Wu S., Zhang X., Duc M., Ho B.* Corrosion of carbon steel influenced by anaerobic biofilm in natural seawater // Electrochim. Acta. — 2008. — **54**, Is. 1. — P. 22—28.
14. *Génin J.-M.R., Ruby C.* Anion and cation distributions in Fe(II–III) hydroxysalt green rusts from XRD and Mössbauer analysis (carbonate, chloride, sulphate, ...); the "fougerite" mineral // Solid State Sci. — 2004. — **6**. — P. 705—718.
15. *Génin J.-M.R., Ruby Ch., Gehin A., Refait Ph.* Synthesis of green rusts by oxidation of $Fe(OH)_2$, their products of oxidation and reduction of ferric oxyhydroxides; Eh–pH Pourbaix diagrams // C.R. Geosci. — 2006. — **338**. — P. 433—446.
16. *Génin J.-M.R., Ruby C.* Composition and anion ordering in some FeII–FeIII hydroxysalt green rusts (carbonate, oxalate, methanoate): The fougerite mineral // Solid State Sci. — 2008. — **10**. — P. 244—259.
17. *Hancen H.C.B.* Composition, stabilization, and light absorption of iron(II)–iron(III) hydroxycarbonate ("Green rust") // Clay Miner. — 1989. — **24**. — P. 663—669.
18. *Jambor J.L., Raudsepp M., Mountjoy K.* Mineralogy of permeable reactive barriers for the attenuation of subsurface contaminants // Can. Miner. — 2005. — **43**. — P. 2117—2140.
19. *Lavrynenko O.M., Korol Ya.D., Netreba S.V., Prokopenko V.A.* Kinetic regularity of the formation of Fe(II)–Fe(III) LDH structures (Green Rust) on the steel surface in presence of the $FeSO_4$ and $Fe_2(SO_4)_3$ water solutions // Chemistry, Physics and Technology of Surface. — 2010. — **1**, No 3. — P. 338—342.
20. *Lavrynenko O.M., Kovalchuk V.I., Netreba S.V., Ulberg Z.R.* New rotation-corrosion dispergation method for obtaining of iron-oxygen nanoparticles // Nanostudies. — 2013. — **7**. — P. 295—322.
21. *Lavrynenko O.M., Netreba S.V., Prokopenko V.A., Korol Ya.D.* The influence of the pH value and the cation composition of dispersion medium on the formation of iron-oxygen structures on steel surface // Chemistry, Physics and Technology of Surface. — 2011. — **2**, No 1. — P. 93—100.
22. *Legrand L., Mazerolles L., Chausse A.* The oxidation of carbonate green rust into ferric phases: solid-state reaction or transformation via solution // Geochim. et cosmochim. acta. — 2004. — **68**, No 17. — P. 3497—3507.
23. *Legrand L., Savoye S., Chausse A., Messina R.* Study of oxidation products formed on iron in solutions containing bicarbonate/carbonate // Electrochim. Acta. — 2000. — No 46. — P. 111—117.
24. *Lewis D.G.* Factors influencing the stability and properties of Green Rusts // Adv. Geoecol. — 1997. — **30**. — P. 345—372.
25. *Leygraf C., Graedel T.* Atmospheric Corrosion. — New York : Wiley Intersci., 2000. — 354 p.
26. *O'Loughlin Ed.J., Larese-Casanova Ph., Scherer M., Cook R.* Green Rust Formation from the Bioreduction of γ-FeOOH (Lepidocrocite): Comparison of Several Shewanella Species // Geomicrobiol. J. — 2007. — **24**, Is. 3—4. — P. 211—230.
27. *Ona-Nguema G., Carteret C., Benali O., Abdelmoula M., Génin J.-M.R., Joranda F.* Competitive formation of hydroxycarbonate green rust I vs hydroxysulphate green rust II in Shewanella putrefaciens cultures // Geomicrobiol. J. — 2004. — **21**. — P. 79—90.
28. *Peulon S., Antony H., Legrand L., Chausse A.* Thin layers of iron corrosion products electrochemically deposited on inert substrates: synthesis and behaviour // Electrochim. Acta. — 2004. — **49**. — P. 2891—2899.
29. *Peulon S., Legrand L., Antony H., Chaussé A.* Electrochemical deposition of thin films of green rusts 1 and 2 on inert gold substrate // Electrochim. Commun. — 2003. — **5**. — P. 208—213.

30. *Refait P., Abdelmoula M., Génin J.-M.R.* Mechanisms of formation and structure of green rust one in aqueous corrosion of iron in the presence of chloride ions // Corros. Sci. — 1998. — **40**. — P. 1547—1560.
31. *Srinivasan R., Lin R., Spicer R.L., Davis B.H.* Structural features in the formation of the green rust intermediate and γ-FeOOH // Coll. Surf. A: Physicochem. Eng. Asp. — 1996. — **113**, No 1. — P. 97—105.
32. *Sumoondur A., Shaw S., Ahmed I., Benning L.G.* Green rust as a precursor for magnetite: an *in situ* synchrotron based study // Miner. Mag. — 2008. — **72**, No 1. — P. 201—204.
33. *Takahashi Y., Matsubara E., Suzuki S., Okamoto Y., Komatsu, T., Konishi H., Mizuki J., Waseda Y.* In-situ X-ray Diffraction of Corrosion Products Formed on Iron Surfaces // Mater. Transactions. — 2005. — **46**, No 3. — P. 637—642.
34. *Tamura H.* The role of rusts in corrosion and corrosion protection of iron and steel // Corros. Sci. — 2008. — **50**. — P. 1872—1883.
35. *Tang Z., Hong S., Xiao W., Taylor J.* Characteristics of iron corrosion scales established under blending of ground, surface, and saline waters and their impacts on iron release in the pipe distribution system // Corros. Sci. — 2006. — **48**, No 2. — P. 322—342.
36. *Trolard F., Abdelmoula M., Bourrie G., Humbert B., Génin J.-M.R.* Evidence of the occurrence of a "Green Rust" component in hydromorphic soils. Proposition of the existence of a new mineral: "fougerite" // Compt. Rend. Acad. Sci. Paris. Ser. IIA. — 1996. — No 323. — P. 1015—1022.
37. *Vins J., Zapletal V., Hanousek F.* Preparation and properties of green rust type substances // Coll. Czech. Chem. Com. — 1987. — **52.** — P. 93—102.
38. *Wolthoorn A., Temminghoff E.J.M., van Riemsdijk W.H.* Colloid formation in groundwater by subsurface aeration: characterization of the geo-colloids and their counterparts // Appl. Geochem. — 2004. — **19**. — P. 1391—1402.
39. *Zachara J.M., Kukkadapu R.K., Fredrickson J.K., Gorby Y.A., Smith S.* Biomineralization of poorly crystalline Fe(III) oxides by dissimilatory metal reducing bacteria (DMRB) // Geomicrobiol. J. — 2002. — **19**. — P. 179—207.

1. Guignet, A. (1961), *Rentgenografija kristallov*, Fizmatgiz, Moskva, 604 p.
2. Lavrynenko, O.M. (2008), *Nanosistemy, nanomaterialy, nanotehnologii*, Kyiv, No 6, pp. 529-550.
3. Lavrynenko, O.M. (2013), *Oderzhannya kompozitsiinikh strukturovanikh sistem na osnovi ferum-oksigenvmisnikh mineraliv, їkh struktura ta vlastivosti,* Avtoref. dys. kand. himicheskih nauk, Kyiv, 40 p.
4. Lurie, Yu.Yu.(1989), *Spravochnik po analiticheskoj himii*, Himija, Moskva, 448 p.
5. Prokopenko, V.A., Lavrynenko, O.M., Vashchenko, O.O. and Nadel, L.G. (2005), *Ekotehnologii i resursosberezhenie*, Kyiv, No 6, pp. 36-42.
6. Evans, Yu.R. (1962), *Korrozija i okislenie metallov (Teoreticheskie osnovy i ih prakticheskoe primenenie),* Mashgiz, Moskva, 856 p.
7. Yung, L. (1967), *Anodnye oksidnye plenki,* Energija, Leningrad, 232 p.
8. Allmann, R. (1968), *Acta Crystallogr. B.*, Vol. 24, pp. 972-977.
9. Allmann, R. and Jepsen, H.P. (1969), *Neues Jahrb. Mineral. Monatsh.*, Vol. 12, pp. 544-551.
10. Antony, H., Peulon, S., Legrand, L., and Chausse, A. (2004), *Electrochim. Acta.*, Vol. 50, pp. 1015-1021.
11. Bernal, J.D., Dasgupta, D. R. and Mackay, A.L. (1959), *Clay Miner. Bull.*, Vol. 4, pp. 15-30.
12. Bigham, J.M., Carlson, L., Murad, E., Winland, R.L. and Wolf, M. (1994), *Miner. Mag.*, Vol. 58, pp. 641-648.
13. Duan, J., Wu, S., Zhang, X., Huangb, G., Duc, M. and Ho, B. (2008), *Electrochim. Acta.*, Vol. 54 No 1, pp. 22-28.
14. Génin, J.-M.R. and Ruby, C. (2004), *Solid State Sci.*, No 6, pp. 705-718.
15. Génin, J.-M.R., Ruby, C., Gehin, A. and Refait, Ph. (2006), *C.R. Geosci.*, No 338, pp. 433-446.
16. Génin, J.-M.R., Ruby, C. (2008), *Solid State Sci.*, No 10, pp. 244-259.
17. Hancen, H.C.B. (1989), *Clay Miner.*, Vol. 24, pp. 663-669.
18. Jambor, J.L., Caudsepp, M. and Mountjoy, K. (2005), *Can. Miner.*, No 43, pp. 2117-2140.
19. Lavrynenko, O.M., Korol, Ya.D., Netreba, S.V. and Prokopenko, V.A. (2010), *Chemistry, Physics and Technology of Surface*, Vol. 1 No 3, pp. 338-342.
20. Lavrynenko, O.M., Kovalchuk, V.I., Netreba, S.V. and Ulberg, Z.R. (2013), *Nanostudies*, No 7, pp. 295-322.
21. Lavrynenko, O.M., Netreba, S.V., Prokopenko, V.A. and Korol, Ya.D. (2011), *Chemistry, Physics and Technology of Surface*, Vol. 2 No 1, pp 93-100.
22. Legrand, L., Mazerolles, L. and Chausse, A. (2004), *Geochim. et cosmochim. acta.*, Vol. 68 No 17, pp. 3497-3507.
23. Legrand, L., Savoye, S., Chausse, A. and Messina, R. (2000), *Electrochim. acta.*, No 46, pp. 111-117.
24. Lewis, D.G. (1997), *Adv. Geoecol.*, Vol. 30, pp. 345-372.
25. Leygraf, C. and Graedel, T. (2000), *Atmospheric Corrosion*, Wiley Intersci., New York, 354 p.
26. O'Loughlin, Ed.J., Larese-Casanova, Ph., Scherer, M. and Cook, R. (2007), *Geomicrobiol. J.*, Vol. 24 No 3-4, pp. 211-230.
27. Ona-Nguema, G., Carteret, C., Benali, O., Abdelmoula, M., Génin, J.-M.R. and Joranda, F. (2004), *Geomicrobiol. J.*, No 21, pp. 79-90.
28. Peulon, S., Antony, H., Legrand, L. and Chaussé, A. (2004), *Electrochim. Acta.*, No 49, pp. 2891-2899.
29. Peulon, S., Legrand, L., Antony H. and Chaussé, A. (2003), *Electrochim. Commun.*, No 5, pp. 208-213.
30. Refait, P., Abdelmoula, M., and Génin, J.-M.R. (1998), *Corros. Sci.*, No 40, pp. 1547-1560.
31. Srinivasan, R., Lin, R., Spicer, R.L. and Davis, B.H. (1996), *Coll. Surf. A: Physicochem. Eng. Asp.*, Vol. 113 No 1. pp. 97-105.

32. Sumoondur, A., Shaw, S., Ahmed, I. and Benning, L.G. (2008), *Miner. Mag.*, Vol. 72 No 1, pp. 201-204.
33. Takahashi, Y., Matsubara, E., Suzuki, Sh., Okamoto, Y., Komatsu, T., Konishi, H., Mizuki, J. and Waseda, Y. (2005), *Mater. Transactions.*, Vol. 46 No 3, pp. 637-642.
34. Tamura, H. (2008), *Corros. Sci.*, No 50, pp. 1872-1883.
35. Tang, Z., Hong, S., Xiao, W. and Taylor, J. (2006), *Corros. Sci.*, Vol. 48 No 2, pp. 322-342.
36. Trolard, F., Abdelmoula, M., Bourrie G., Humbert, B. and Genin, J.-M.R. (1996), *Compt. Rend. Acad. Sci.* Paris, Ser. IIA, No 323, pp. 1015-1022.
37. Vins, J., Zapletal, V. and Hanousek, F. (1987), *Coll. Czech. Chem. Com.,* No 52, pp. 93-102.
38. Wolthoorn, A., Temminghoff, E.J.M. and van Riemsdijk, W.H. (2004), *Appl. Geochem*, No 19, pp. 1391-1402.
39. Zachara, J.M., Kukkadapu, R.K., Fredrickson, J.K., Gorby, Y.A. and Smith, S.C. (2002), *Geomicrobiol. J.*, No 19, pp. 179-207.

Received 28.12.2014

О.М. Лавриненко, Ю.С. Щукін

Інститут біоколоїдної хімії ім. Ф.Д. Овчаренка НАН України
03680, м. Київ-142, Україна, бульв. Акад. Вернадського, 42
E-mail: alena-lavry@yandex.ru

РОЗВИТОК ГІДРОКСИКАРБОНАТНОГО *GREEN RUST* НА ПОВЕРХНІ СТАЛІ, ЯКА КОНТАКТУЄ З ВОДНИМ ДИСПЕРСІЙНИМ СЕРЕДОВИЩЕМ У ДІАПАЗОНІ ТЕМПЕРАТУРИ ВІД 3 ДО 70 °С

Досліджено вплив pH водного дисперсійного середовища та температури на процес утворення гідроксикарбонатного *Green Rust GR*(CO_3^{2-}) на поверхні сталі за умов ротаційно-корозійного диспергування (РКД). Спираючись на дані рентгенофазового аналізу *in situ* та сканувальної електронної мікроскопії показано залежність морфології частинок лепідокроките та магнетиту від колоїдно-хімічного механізму їх утворення. Встановлено, що в результаті твердофазного перетворення *GR*(CO_3^{2-}) частинки лепідокроките успадковують його платівкоподібну форму, в той час як за розчинення *GR*(CO_3^{2-}) та переосадження продуктів його розчинення частинки лепідокроките набувають голкоподібної форми. Інший продукт розчинення—переосадження *GR*(CO_3^{2-}) — магнетит, який утворюється на прилеглому до поверхні сталі боці окисної плівки і характеризується сферичною формою та нанометровими розмірами частинок. Оптимальні умови формування *GR*(CO_3^{2-}) за умов РКД були зафіксовані після 5 год проходження процесу фазоутворення за pH 11,0 та T = 20 °С і pH ~6,0 та T = 25—35 °С.

Ключові слова: Fe(II)–Fe(III) шаруваті подвійні гідроксиди, гідроксикарбонатний *Green Rust*, лепідокроките, магнетит, поверхня сталі, умови ротаційно-корозійного диспергування.

Е.Н. Лавриненко, Ю.С. Щукин

Институт биоколлоидной химии им. Ф.Д. Овчаренко НАН Украины
03680, г. Киев-142, Украина, бульв. Акад. Вернадского, 42
E-mail: alena-lavry@yandex.ru

РАЗВИТИЕ ГИДРОКСИКАРБОНАТНОГО *GREEN RUST* НА ПОВЕРХНОСТИ СТАЛИ, КОНТАКТИРУЮЩЕЙ С ВОДНОЙ ДИСПЕРСИОННОЙ СРЕДОЙ В ДИАПАЗОНЕ ТЕМПЕРАТУРЫ ОТ 3 ДО 70 °С

Исследовано влияние pH водной дисперсионной среды и температуры на процесс формирования гидроксикарбонатного *Green Rust GR*(CO_3^{2-}) на поверхности стали в условиях ротационно-коррозионного диспергирования (РКД). На основании данных рентгенофазового анализа *in situ* и сканирующей электронной микроскопии показана зависимость морфологии частиц лепидокрокита и магнетита от коллоидно-химического механизма их формирования. Установлено, что в результате твердофазной трансформации *GR*(CO_3^{2-}) частицы лепидокрокита наследуют его пластинчатую форму, а при растворении *GR*(CO_3^{2-}) и переосаждении продуктов его растворения частицы лепидокрокита приобретают иглообразную форму. Другой продукт растворения—переосаждения *GR*(CO_3^{2-}) — магнетит, который образуется на прилегающей к поверхности стали стороне окисной пленки и характеризуется сферической формой и нанометровыми размерами частиц. Оптимальные условия формирования *GR*(CO_3^{2-}) на поверхности стали в условиях РКД зафиксированы после пятичасового прохождения процесса фазообразования при pH 11,0 и T = 20 °С, а также pH ~6,0 и T = 25—35 °С.

Ключевые слова: Fe(II)–Fe(III) слоистые двойные гидроксиды, гидроксикарбонатный *Green Rust*, лепидокрокит, магнетит, поверхность стали, условия ротационно-коррозионного диспергирования.